Supplement of

The influence of mixing on stratospheric circulation changes in the 21st century

R. Eichinger et al.

Correspondence to: R. Eichinger (roland.eichinger@dlr.de)

1 Introduction

This supplement contains additional material to the article *"The influence of mixing on stratospheric circulation changes in the 21st century"*. We provide additional figures for Sect. 3.4 of the paper. In the main article, the multi-model-means of eight model simulations of the zonal wind $\overline{u}$, the Eliassen-Palm flux divergence, the meridonal residual circulation v^*, the meridional PV-gradient ($\partial PV/\partial y$), the diffusivity coefficient K_{yy} and the ratio $K_{yy}/|v^*|$ are given. Here, we show these quantities for each of the eight CCMI-1 (Chemistry Climate Model Intercomparison project) REF-C2 model simulations individually. The models that were used in this analysis are ACCESS, CMAM, EMAC-L47, EMAC-L90, GEOSCCM, MRI, NIWA-UKCA and WACCM. For more information on these models, the simulation setup and the selection of the models, see main article.

2 Additional figures

ACCESS

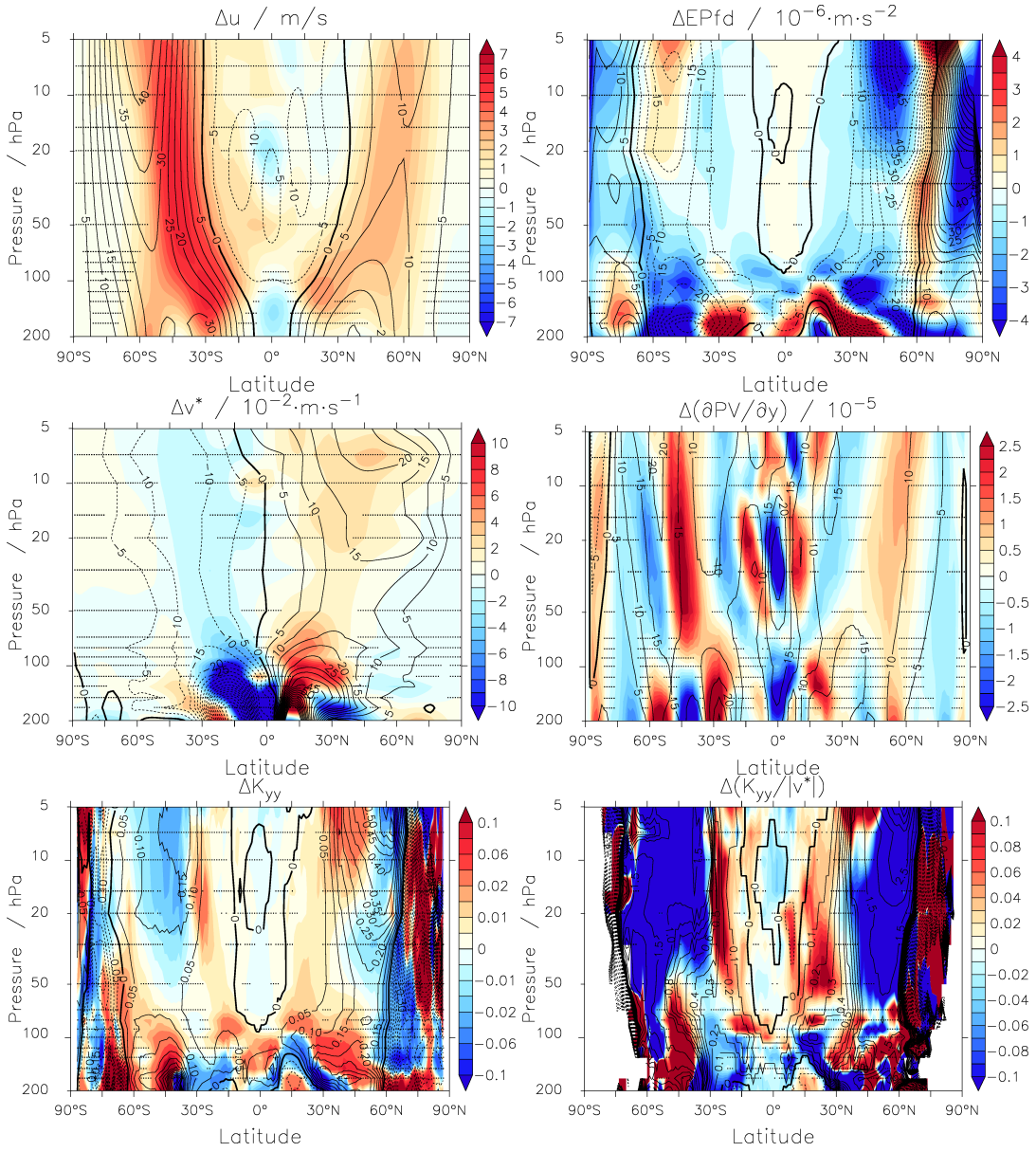

Figure 1. ACCESS CCMI REF-C2 model simulation differences (Δ) of (a) the zonal wind $\overline{u}$, (b) the EP flux divergence, (c) the meridonal residual circulation v*, (d) the meridional PV-gradient ($\partial PV/\partial y$), (e) the diffusivity coefficient K_{yy} and (f) the ratio $K_{yy}/|v^*|$ between the periods 1970-1990 and 2080-2100. The contour lines show the multi-model mean climatology of the first period of the respective quantity. Stippled regions show where the statistical significance of the difference is below the threshold 95%.

CMAM

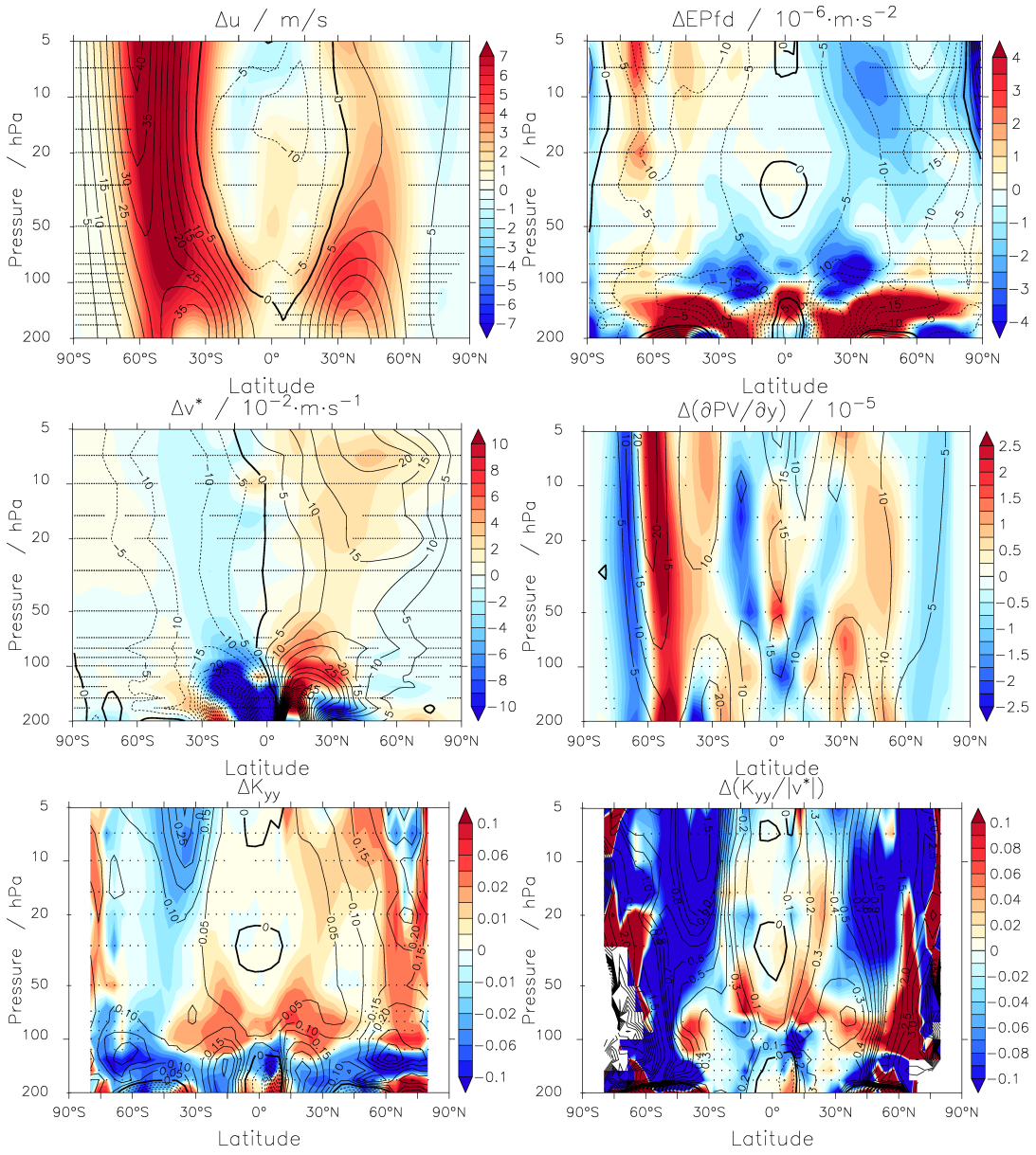

Figure 2. CMAM CCMI REF-C2 model simulation differences (Δ) of (a) the zonal wind $\overline{u}$, (b) the EP flux divergence, (c) the meridonal residual circulation v*, (d) the meridional PV-gradient ($\partial PV/\partial y$), (e) the diffusivity coefficient K_{yy} and (f) the ratio $K_{yy}/|v^*|$ between the periods 1970-1990 and 2080-2100. The contour lines show the multi-model mean climatology of the first period of the respective quantity. Stippled regions show where the statistical significance of the difference is below the threshold 95%.

EMAC-L47

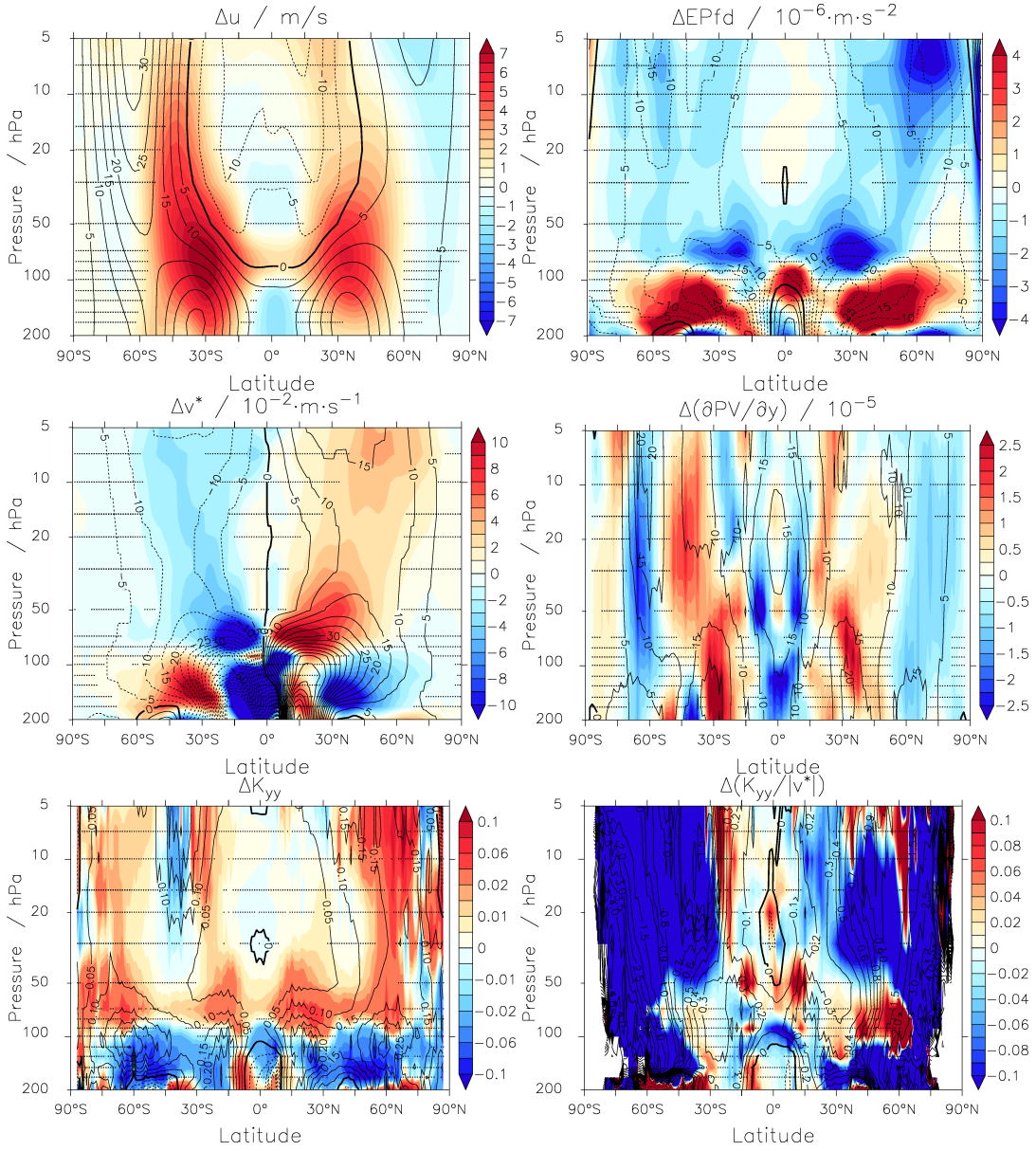

Figure 3. EMAC-L47 CCMI REF-C2 model simulation differences (Δ) of (a) the zonal wind $\overline{u}$, (b) the EP flux divergence, (c) the meridonal residual circulation v*, (d) the meridional PV-gradient ($\partial PV/\partial y$), (e) the diffusivity coefficient K_{yy} and (f) the ratio $K_{yy}/|v^*|$ between the periods 1970-1990 and 2080-2100. The contour lines show the multi-model mean climatology of the first period of the respective quantity. Stippled regions show where the statistical significance of the difference is below the threshold 95%.

EMAC-L90

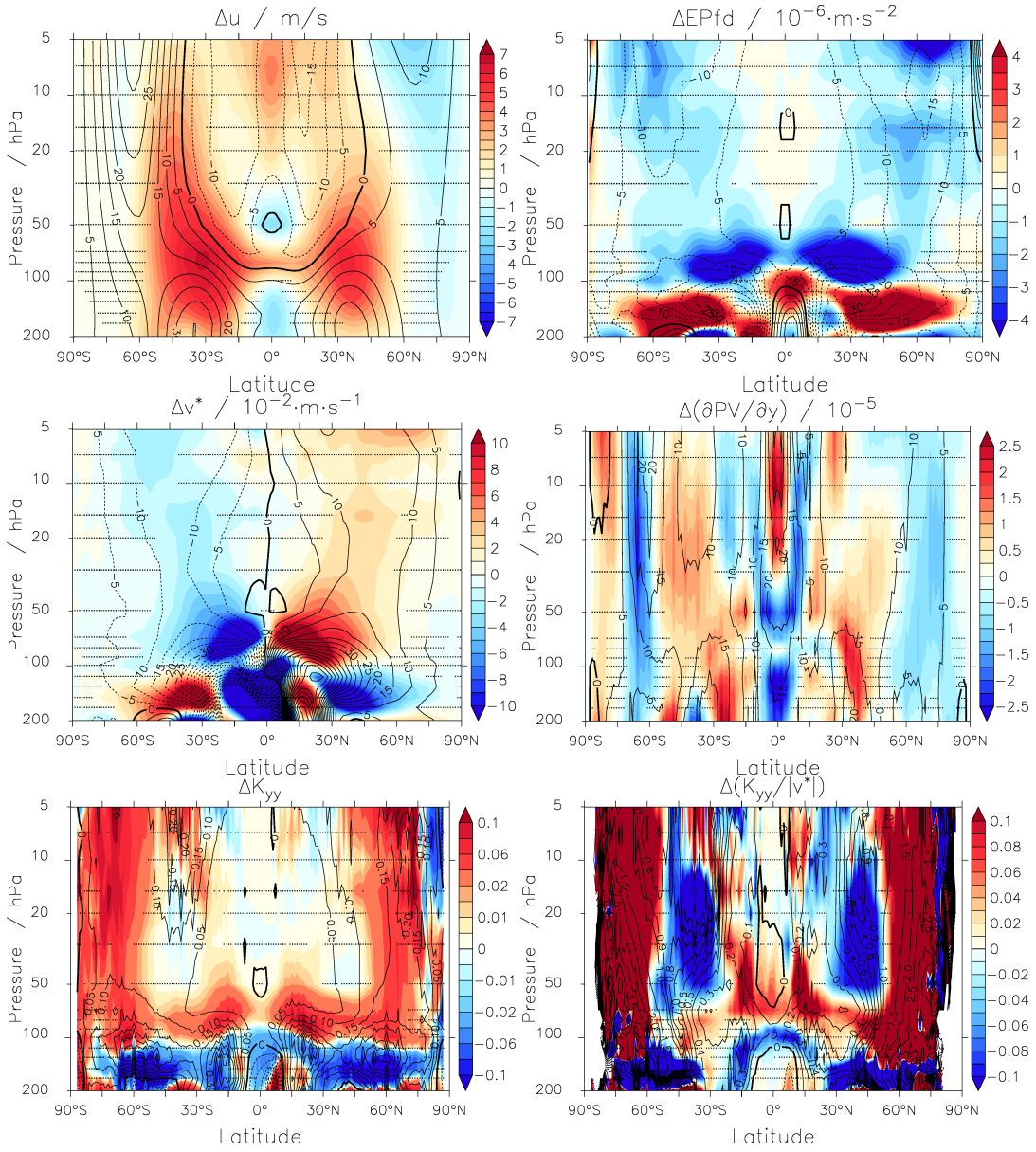

Figure 4. EMAC-L90 CCMI REF-C2 model simulation differences (Δ) of (a) the zonal wind $\overline{u}$, (b) the EP flux divergence, (c) the meridonal residual circulation v*, (d) the meridional PV-gradient ($\partial PV/\partial y$), (e) the diffusivity coefficient K_{yy} and (f) the ratio $K_{yy}/|v^*|$ between the periods 1970-1990 and 2080-2100. The contour lines show the multi-model mean climatology of the first period of the respective quantity. Stippled regions show where the statistical significance of the difference is below the threshold 95%.

GEOSCCM

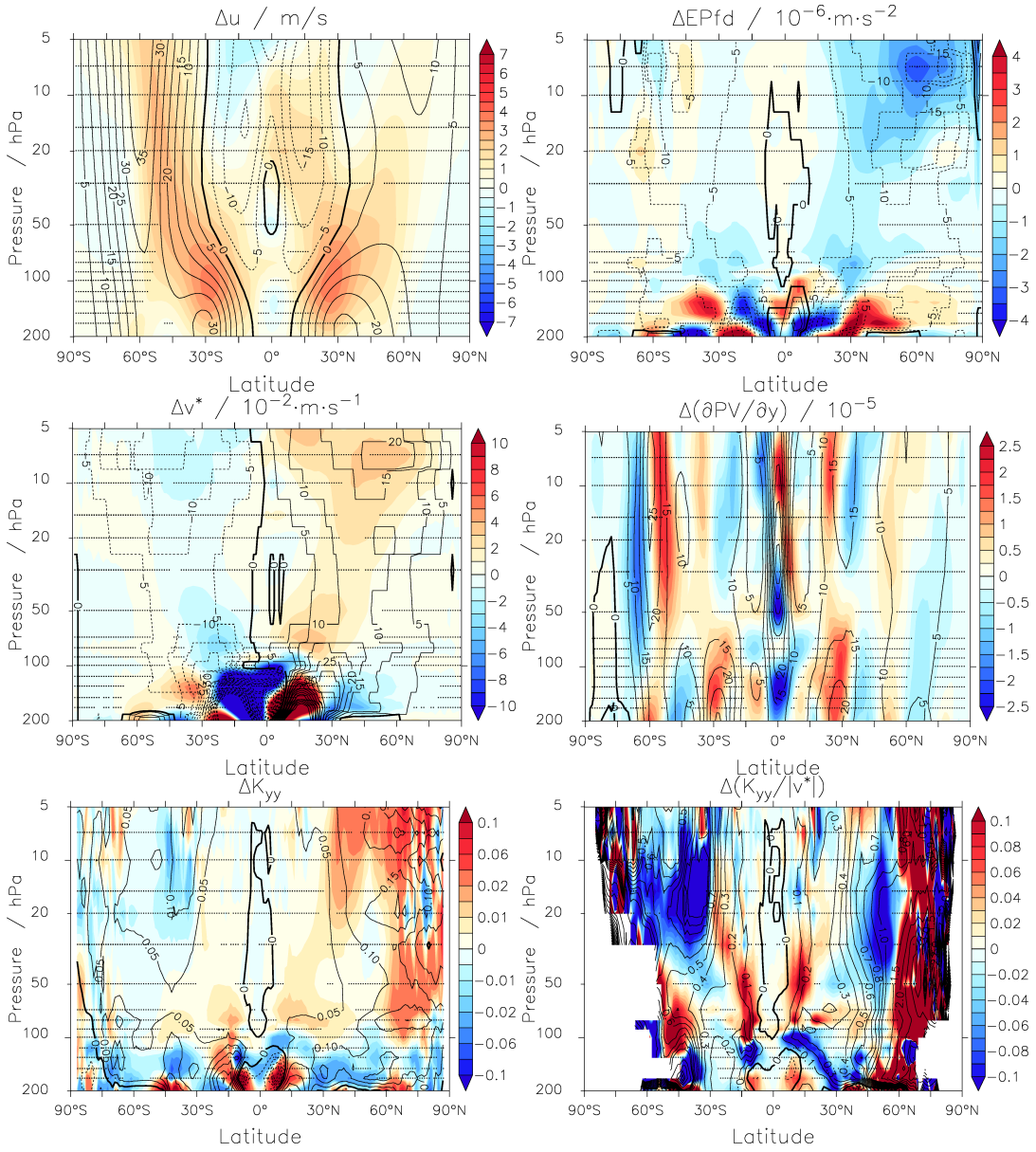

Figure 5. GEOSCCM CCMI REF-C2 model simulation differences (Δ) of (a) the zonal wind $\overline{u}$, (b) the EP flux divergence, (c) the meridonal residual circulation v*, (d) the meridional PV-gradient ($\partial PV/\partial y$), (e) the diffusivity coefficient K_{yy} and (f) the ratio $K_{yy}/|v^*|$ between the periods 1970-1990 and 2080-2100. The contour lines show the multi-model mean climatology of the first period of the respective quantity. Stippled regions show where the statistical significance of the difference is below the threshold 95%.

MRI

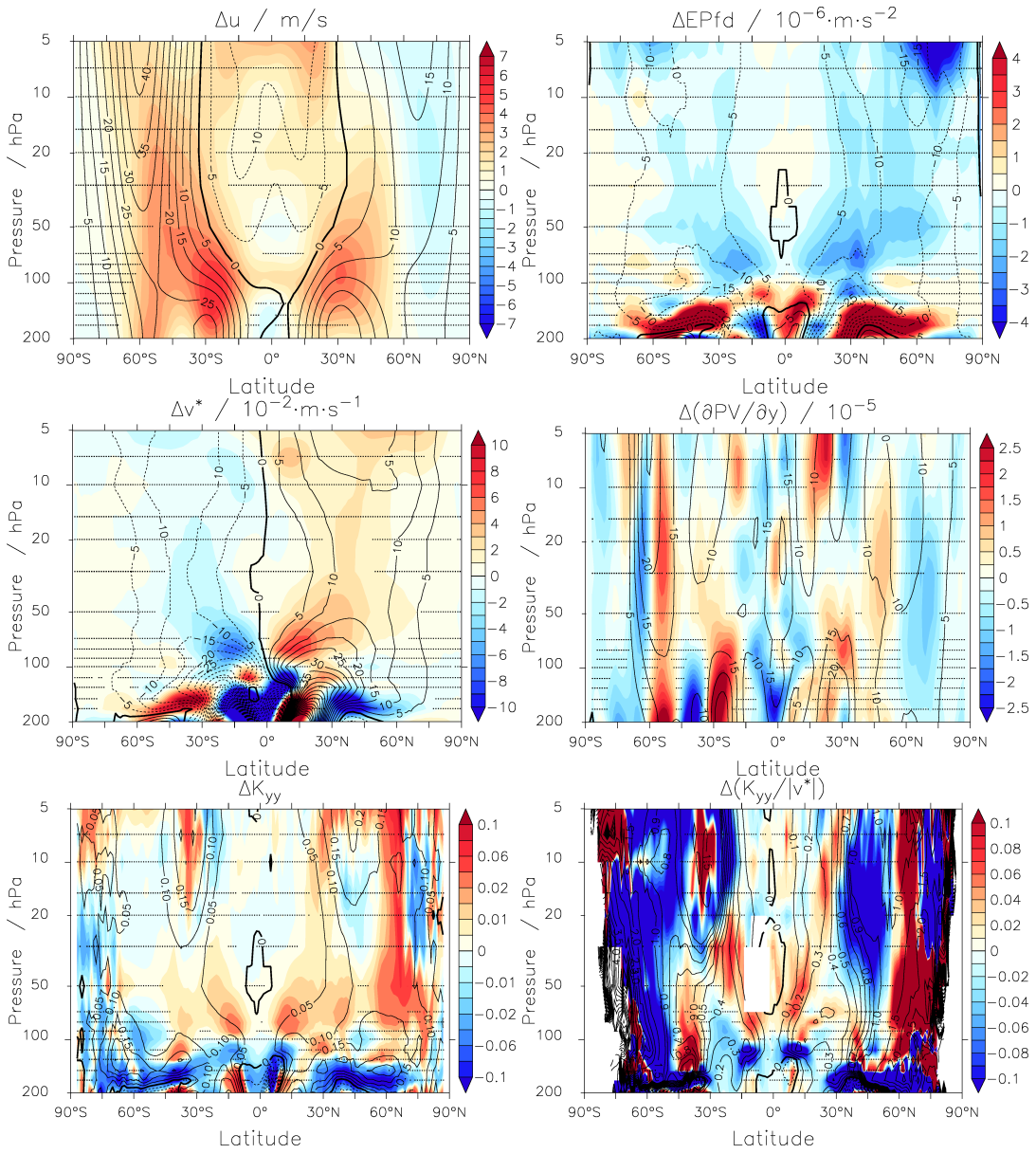

Figure 6. MRI CCMI REF-C2 model simulation differences (Δ) of (a) the zonal wind $\overline{u}$, (b) the EP flux divergence, (c) the meridonal residual circulation v*, (d) the meridional PV-gradient ($\partial PV/\partial y$), (e) the diffusivity coefficient K_{yy} and (f) the ratio $K_{yy}/|v^*|$ between the periods 1970-1990 and 2080-2100. The contour lines show the multi-model mean climatology of the first period of the respective quantity. Stippled regions show where the statistical significance of the difference is below the threshold 95%.

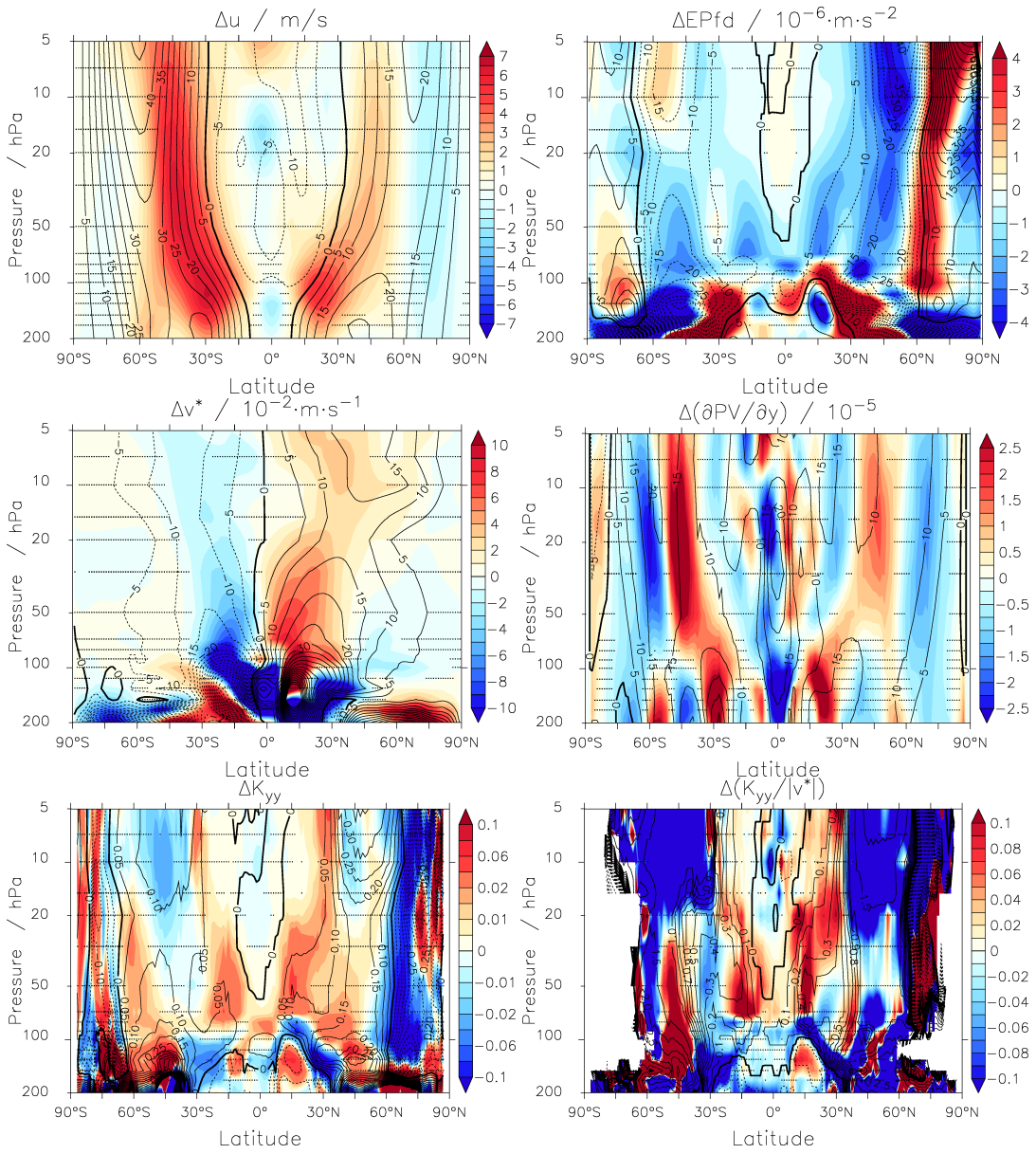

Figure 7. NIWA-UKCA CCMI REF-C2 model simulation differences (Δ) of (a) the zonal wind $\overline{u}$, (b) the EP flux divergence, (c) the meridonal residual circulation v*, (d) the meridional PV-gradient ($\partial PV/\partial y$), (e) the diffusivity coefficient K_{yy} and (f) the ratio $K_{yy}/|v^*|$ between the periods 1970-1990 and 2080-2100. The contour lines show the multi-model mean climatology of the first period of the respective quantity. Stippled regions show where the statistical significance of the difference is below the threshold 95%.

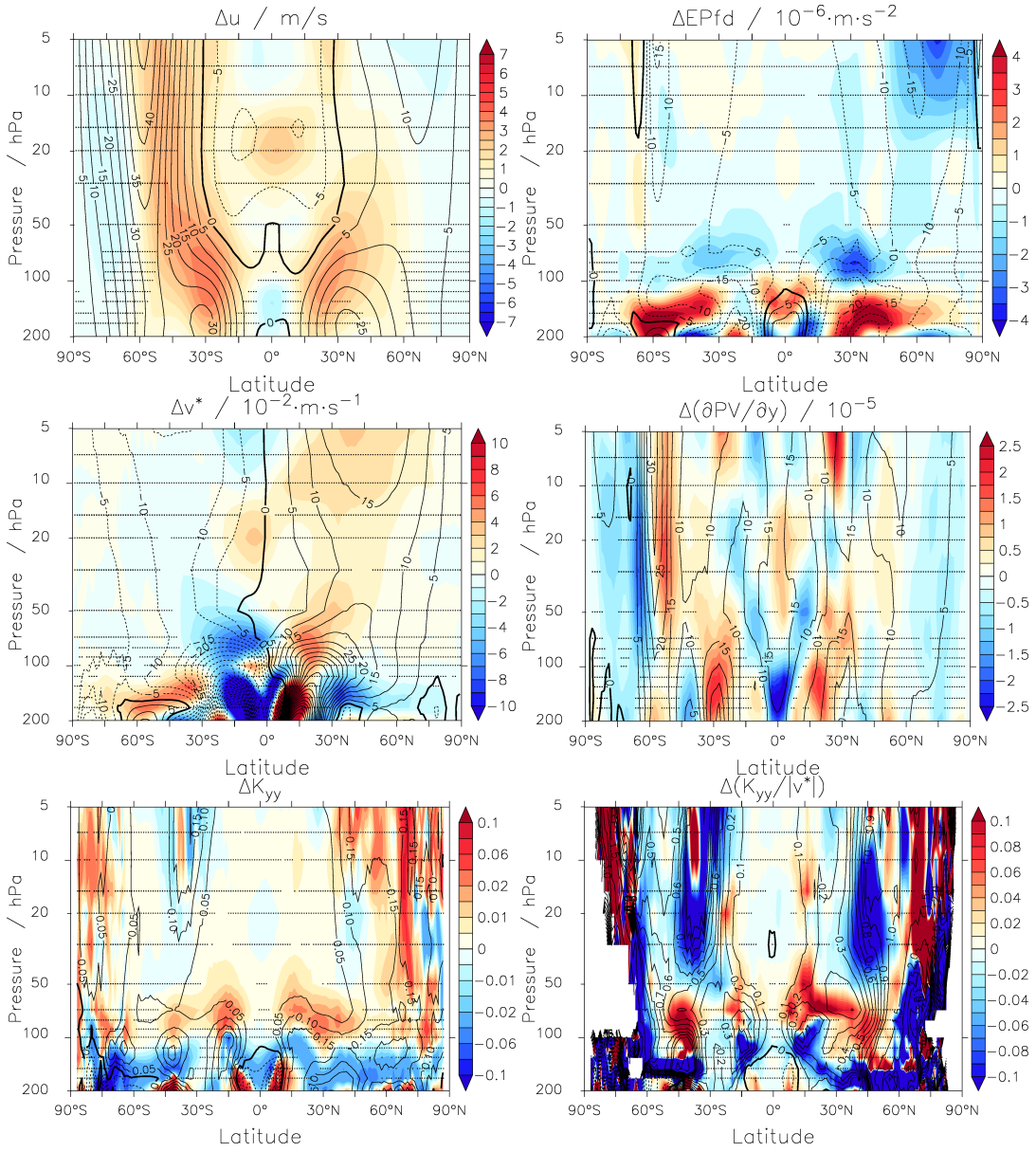

Figure 8. WACCM CCMI REF-C2 model simulation differences (Δ) of (a) the zonal wind $\overline{u}$, (b) the EP flux divergence, (c) the meridonal residual circulation v*, (d) the meridional PV-gradient ($\partial PV/\partial y$), (e) the diffusivity coefficient K_{yy} and (f) the ratio $K_{yy}/|v^*|$ between the periods 1970-1990 and 2080-2100. The contour lines show the multi-model mean climatology of the first period of the respective quantity. Stippled regions show where the statistical significance of the difference is below the threshold 95%.